Nanoscale

PAPER

View Article Online
View Journal | View Issue

Published on 05 February 2015. Downloaded by University of California - Santa Barbara on 09/02/2016 05:21:11.

Cite this: *Nanoscale*, 2015, **7**, 4929

Application of tungsten as a carbon sink for synthesis of large-domain uniform monolayer graphene free of bilayers/multilayers†

Wenjing Fang,[a] Allen Hsu,[a] Yong Cheol Shin,[b] Albert Liao,[a] Shengxi Huang,[a] Yi Song,[a] Xi Ling,[a] Mildred S. Dresselhaus,[a,c] Tomas Palacios[a] and Jing Kong*[a]

Received 15th December 2014,
Accepted 4th February 2015

DOI: 10.1039/c4nr07418a

www.rsc.org/nanoscale

We have found that tungsten (W) foils can be used for controlling the carbon diffusion within copper (Cu) enclosures to synthesize large-domain bi-/multi-layer-free monolayer graphene *via* chemical vapor deposition. We have observed that bi-/multi-layer graphene that nucleate underneath the monolayer graphene can be selectively removed by a W foil placed inside of the Cu enclosure. Both X-ray photoelectron spectroscopy and X-ray diffraction reveal the formation of tungsten sub-carbide (W_2C), suggesting the role of the W foil as a carbon sink that alters the carbon concentration inside of the enclosure. Consequently, the bi-/multi-layers appear to dissolve. Utilizing this selective removal process, we were able to demonstrate large-domain (>200 μm) monolayer graphene that is free of any bi-/multi-layers by using Cu double enclosures.

Introduction

Chemical vapor deposition (CVD) offers great potential for synthesizing high-quality large-area graphene that can be transferred onto arbitrary substrates.[1–4] In particular, large-domain graphene (>100 μm) has been achieved with a quality comparable to that of exfoliated graphene using a Cu enclosure.[5,6] This approach has enabled the synthesis of graphene under low CH_4 conditions to achieve extremely low nucleation densities.[5] Unfortunately, while reducing the carbon flow significantly, the enclosure method often results in the formation of bi-/multi-layers in the film.[5,7] Under these low growth rate conditions, there are more surface edges available in the monolayer graphene for the diffusion of carbon underneath the monolayer to form bi-/multi-layers.[8,9] As a consequence, large monolayer domains and large bi-/multi-layer domains (20 μm–100 μm) always appear hand-in-hand. However, the different electronic properties of bi-/multi-layers can reduce the homogeneity and transport of electronic carriers within the monolayer graphene.[10,11] To achieve uniform monolayer graphene, various methods have been explored, such as tuning growth conditions[7,12] and pretreating the Cu using etchant cleaning, electro-chemically polishing, and many-hour annealing.[13–15] Nevertheless, bi-/multi-layers can still be observed very often.[7,12,16–18] On the other hand, we can suppress the size of the bilayers of graphene through a faster growth rate of monolayer graphene by applying a higher CH_4 concentration, but the monolayer domain size will then be compromised.[7] As a result, techniques to circumvent the competition between monolayer domain size and layer uniformity are required.

In this work, we have focused on graphene growth on Cu enclosures due to the asymmetry between the growth mechanisms of monolayer and bi-/multi-layer graphene.[19] Our previous work has shown that by using Cu enclosures for graphene synthesis, a high coverage of bilayer graphene can be achieved on the outside surface of the enclosure because carbon species on the inside can diffuse out to form bilayers on the outside.[19,20] The carbon diffusion process is driven by the concentration gradient across the Cu foil. Here, we reverse the direction of the carbon diffusion by placing a carbon sink (W foil) on the inside of the enclosure, and found that bi-/multi-layers can be selectively removed from the outside surface so that uniform monolayer graphene is then obtained.

Experimental

Cu foil (99.9%, 127 μm) and W foil (99.95%, 50 μm) were purchased from Alfa Aesar. Tungsten carbide (WC, ≥99%) was purchased from Sigma Aldrich. The preparations of the Cu enclosure and the transfer process were described in our pre-

[a]*Department of Electrical Engineering and Computer Sciences, Cambridge, Massachusetts 02139, USA. E-mail: jingkong@mit.edu*
[b]*Department of Material Science and Engineering, Cambridge, Massachusetts 02139, USA*
[c]*Department of Physics, Massachusetts Institute of Technology, Cambridge, Massachusetts 02139, USA*
†Electronic supplementary information (ESI) available. See DOI: 10.1039/c4nr07418a

Published on 05 February 2015. Downloaded by University of California - Santa Barbara on 09/02/2016 05:21:11.

vious work.[19,20] All samples were grown at 1045 °C under 1 sccm CH_4 and 50 sccm H_2. We present false colored optical images in order to highlight the bilayer regions. The bare SiO_2 surface is shown in white, while the different thicknesses of graphene films are represented in different shades of pink. Raman mapping was performed in a home built Raman system with an X–Y motorized microscope stage and an Nd: YAG laser at 532 nm at a power of ~1–2 mW using a 100× objective and a beam spot size of ~1 μm. Data were then processed with automated Lorentzian fitting in MATLAB. X-ray photoelectron spectroscopy (XPS) was performed using a PHI Versaprobe II. X-ray diffraction (XRD) was performed using a Panalytical Multipurpose Diffractometer with Cu Kα radiation. Selected area diffraction patterns (SAED) were then taken using a JEOL 2011 transmission electron microscope at 120 kV. The size for SAED was 100 nm.

Results and discussion

Fig. 1 shows the optical images of the transferred graphene films (on SiO_2/Si substrates) grown on a flat Cu foil, an empty Cu enclosure, and a Cu enclosure with a W foil inside (illustrations shown in the insets). In Fig. 1a, small bilayers can be observed on the flat Cu foil, due to the diffusion of carbon atoms underneath the first grown monolayer at the nucleation stage.[8,19] On the other hand, monolayer graphene with high-coverage bi-/multi-layers appears on the outside of the empty Cu enclosure in Fig. 1b, which is consistent with our previous report[19] (see Raman spectra in ESI†). For a typical graphene growth on a Cu enclosure, the carbon can leak slowly into the inside of the enclosure through the gaps at the edges, forming a carbon source on the inside, which can diffuse out to form bi-/multi-layers.[19] However, for Cu enclosures with a piece of W foil enclosed, there is no graphene growth on the inside of the enclosure. This observation suggests that the carbon supply to the monolayer graphene is reduced by the W foil. In addition, it has been reported that the presence of the W foil does not interfere with the growth of graphene on Cu,[21] nor does W interdiffuse into Cu.[22] At the same time, the graphene on the outside surface is uniform with no bi-/multi-layers present in Fig. 3c. This indicates that there is no available carbon source provided from the inside of the enclosure, in agreement with the observation that no graphene forms on the inside.

To investigate the growth mechanism of uniform monolayer graphene, we compare in Fig. 2 the graphene films grown on

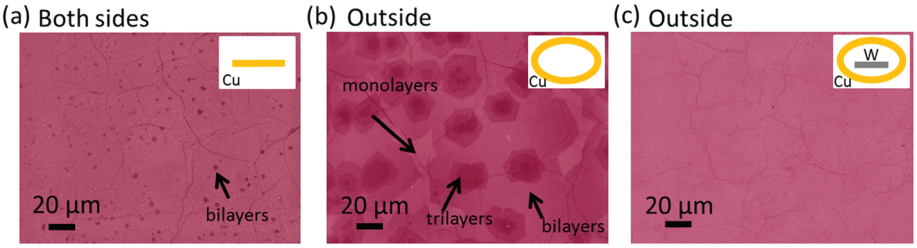

Fig. 1 Optical images of graphene grown on (a) a flat Cu foil, (b) the outside surface of the Cu enclosure and (c) the outside surface of the Cu enclosure with a W foil inside. The different thicknesses of graphene are represented by different shades of pink. The darker regions are bilayers or multilayers.

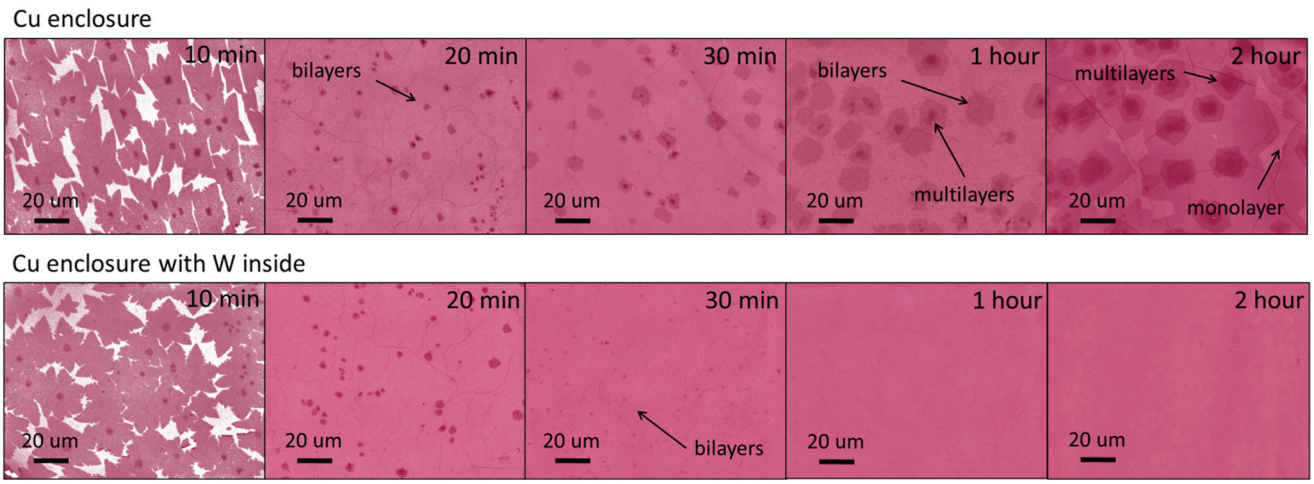

Fig. 2 Optical images of transferred graphene grown on the outside of the Cu enclosure as a function of time. On the outside surface of the Cu enclosure, the bilayer growth on the outside continues to grow. In contrast, bilayers grow during the first 20 minutes but start to disappear on the Cu enclosure with a W foil inside. The monolayer graphene film remains uniform for the rest of the growth time of up to 2 hours.

 This journal is © The Royal Society of Chemistry 2015

Published on 05 February 2015. Downloaded by University of California - Santa Barbara on 09/02/2016 05:21:11.

the outside of the Cu enclosures with and without W enclosed for different times. For the first 10 min, bi-/multi-layers indeed nucleate in the center of the monolayer graphene flakes on both of the Cu enclosures.[19] As time progresses, for the empty Cu enclosure, the monolayer becomes complete and the bi-/multi-layers continue to grow larger due to the continuous flow of carbon from the inside of the enclosure. In contrast, for the Cu enclosure with the W foil, the bi-/multi-layers start to diminish in size and eventually disappear after one hour. In addition, high resolution scanning electron microscopy (SEM) images also confirm that the graphene on the Cu enclosure with W foil enclosed is a uniform monolayer with no bi-/multi-layers (see ESI†). At the same time, no graphene grows on the inside, indicating that the concentration of carbon sources is extremely low.[23] However, when we grow graphene under the same conditions for five hours, bi-/multi-layers start to appear again on the outside and graphene grows on the inside simultaneously (see ESI†).

Since the bi-/multi-layers grow at the beginning and then disappear later, a question arises: is the monolayer graphene also affected by the W? To answer this question, we have utilized carbon isotopes ($^{13}CH_4$ and $^{12}CH_4$) to identify the carbon incorporation as a function of time. We grew graphene by sequentially flowing $^{13}CH_4$ for the first 15 min and then $^{12}CH_4$ for the remaining time using a Cu enclosure with W foil inside. Based on the time dependent studies in our previous work, the monolayer and bi-/multi-layers on the outside surface should be solely composed of ^{13}C.[20] If the graphene is being substituted during the growth process by the incoming carbon, ^{12}C will be incorporated into the films. Finally, using Raman spectroscopy, we can locate and differentiate the various carbon isotopes.[24] The positions of Raman peaks are dependent on the masses of ^{12}C and ^{13}C.[25] We thus performed Raman mapping on the graphene grown on the outside surface of the Cu enclosures with W foil enclosed. The G peak position of the monolayer composed of ^{12}C and ^{13}C is located at around 1583 cm^{-1} and 1535 cm^{-1}, respectively.[20] The percentages of ^{12}C and ^{13}C were extracted and plotted in Fig. 3a. The absence of ^{12}C throughout the entire process suggests that the film is completely composed of ^{13}C, implying that under the same growth conditions, no substitution of carbon in the monolayer occurs. Only small bilayer regions grown at the beginning disappear, while the monolayer regions remain intact. This observation is also supported by previous reports that once Cu is fully covered, there is no catalytic surface to further decompose $^{12}CH_4$.[4,26] The difference in the results of the monolayer and small bi-/multi-layers is probably due to the edges of graphene. It is possible that the edges of the small

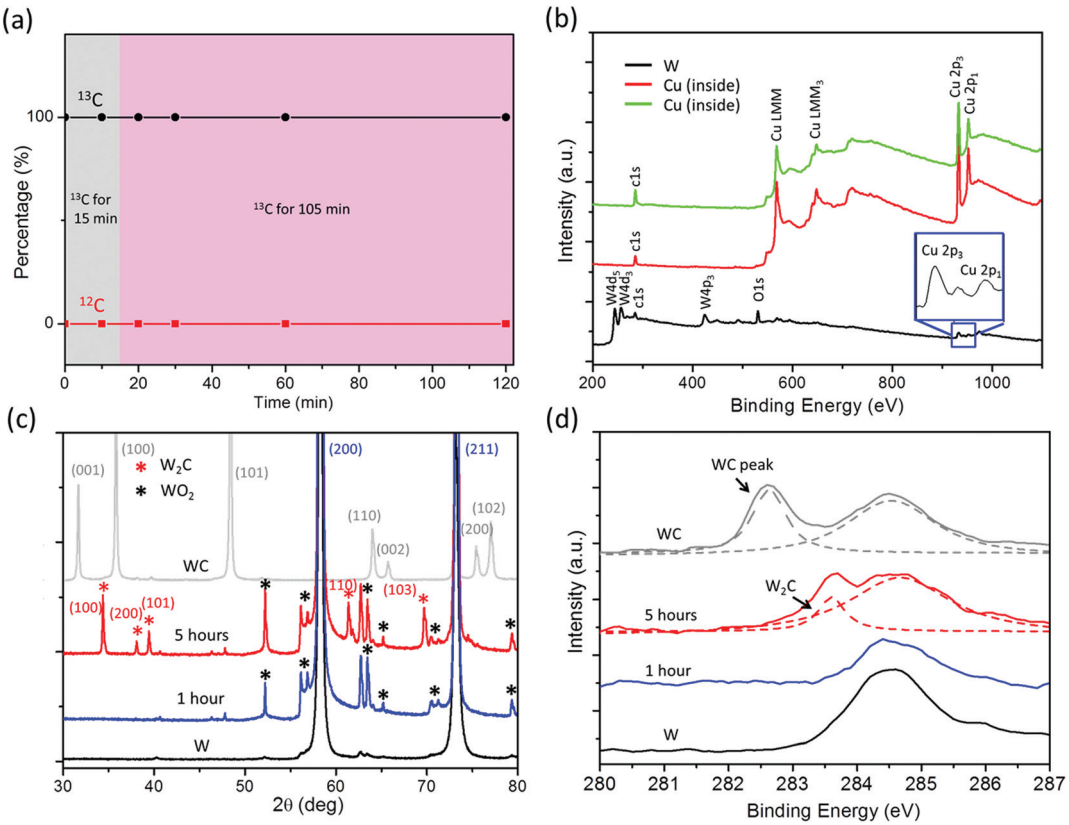

Fig. 3 Characterization of the graphene grown on Cu enclosures with W and the composition analysis of the W foil. (a) Percentage of the ^{12}C and ^{13}C isotope in monolayer graphene grown using isotopic labeling. (b) XPS results on W and on both inside and outside surfaces of the Cu enclosures. (c) XRD results on as-received W foil (black), W foil after 1 hour (blue) and 5 hour growth (red), and as-received WC (grey). (d) A detailed XPS spectrum of C 1s. Fitted peaks are shown with dashed lines.

Published on 05 February 2015. Downloaded by University of California - Santa Barbara on 09/02/2016 05:21:11.

bilayers are unbounded and chemically active.[27,28] With the assistance of the catalytic Cu foil, the reaction of graphene formation is reversed, such that graphene is etched back to carbon, diffuses inwards through the Cu foil, and is eventually consumed by the W foil.[29] In contrast, the edges of monolayer graphene domains are bonded to adjacent grains, thereby making them more stable as compared to that of the bi-/multi-layers.[18,30,31]

To elucidate the role of the W foil, we use a combination of X-ray photoelectron spectroscopy (XPS) and X-ray diffraction (XRD) to study the change of the chemical composition of the W foil. We performed XPS on both the outside and inside surfaces of the Cu enclosure and found that there is no presence of W. On the other hand, there is a presence of Cu on the W foil after 1 hour of growth, as shown in the inset in Fig. 3b. This is expected because the growth process was carried out at 1045 °C, which is close to the melting temperature of Cu, resulting in Cu evaporation on the W foil during the growth process. To show that the thin Cu layer on W does not affect the role of the W, we placed a W foil into a Cu enclosure for annealing under 10 sccm H_2 at 1045 °C for 1 hour. Then, we removed the W foil which had been coated with a thin layer of Cu and repeated our previous growth utilizing a Cu-coated W foil in place of our standard W foil. For the same growth conditions, we found that uniform monolayer graphene can still be obtained (see ESI†). Fig. 3c shows the XRD results on as-received W (without any growth), W after one hour growth (inside the Cu enclosure), W after five hours growth and as-received WC, respectively. In Fig. 3c, for W after five hour growth, the W_2C peaks are evident, as highlighted by red asterisks. Formation of WC was reported by annealing graphene oxide and tungsten oxide;[32] however, here we found W_2C forms on the W under our growth conditions. Moreover, recent research has shown that W_2C is stable even at high temperature and with more carbon source provided.[33–36] The formation of W_2C indicates that the carbon source is slowly being incorporated into the W. Nevertheless, the W_2C peak is not observed after only one hour growth. This can be explained by the fact that there are no significant amounts of detectable W_2C present due to the low carbon concentration on the inside at the beginning of the growth process.[5,19] In Fig. 3d, high resolution XPS of C 1s confirms the presence of W_2C, located at 283.6 eV, which can be distinguished from WC at 282.6 eV.[37,38] All the peaks are fitted with Gaussian functions of different widths. The peak located at around 284.6 eV with full width half maximum (FWHM) larger than 1 eV is from the presence of adventitious carbon adsorbed on the surface, instead of graphene or graphite formation. For graphene or graphite, the FWHM of the peak is much narrower (<1 eV).[39]

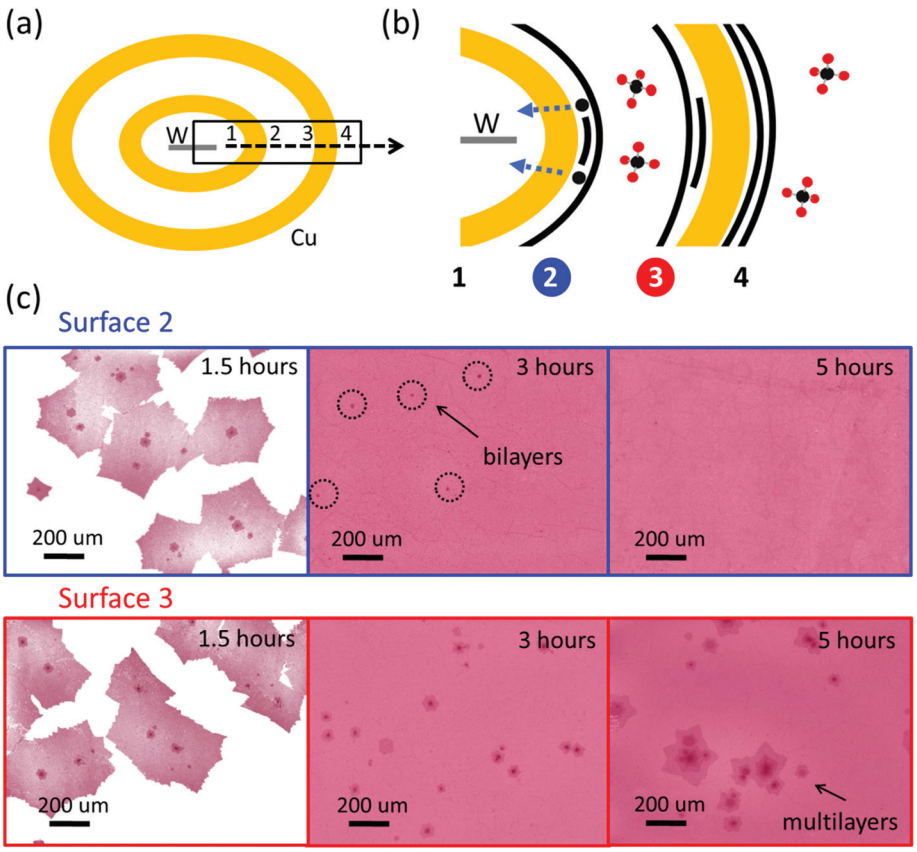

Fig. 4 Graphene grown on Cu double enclosures. (a) Schematics of the Cu double enclosures. (b) Growth mechanism for bi-/multi-layer graphene on surface 2 disappears while growth remains on surface 3. (c) Comparison of graphene grown on surfaces 2 and 3 as a function of time.

 This journal is © The Royal Society of Chemistry 2015

Published on 05 February 2015. Downloaded by University of California - Santa Barbara on 09/02/2016 05:21:11.

Since the W foil removes the bilayer graphene from the outer surface of an enclosure, we can utilize this method for preparing large-domain bi-/multi-layers-free graphene using a Cu double enclosure geometry. The schematics of the Cu double enclosure are shown in Fig. 4a. The W foil is placed inside the small Cu enclosure, which itself is placed inside a larger Cu enclosure. The surfaces on both sides of the Cu enclosures are numbered from the inside to outside. For example, the innermost surface of the small enclosure is labeled surface 1 and the outside surface of the big enclosure is labeled surface 4. After growth under the same conditions for different lengths of time, graphene films on surface 2 and 3 were transferred and compared. After 1.5 hours, the domain size of graphene is more than 200 μm. In the center of the domains, we can find bi-/multi-layers. As time proceeds, monolayer graphene is complete and bi-/multi-layers graphene continue to grow larger on surface 3 (highlighted in red). In contrast, the bi-/multi-layers on surface 2 start to disappear, resulting in a uniform monolayer. Both surfaces 2 and 3 are exposed to the same environment with the same gas composition and temperature. However, because of the presence of a W foil inside the small Cu enclosure, the bi-/multi-layers underneath surface 2 can be removed, consistent with earlier observations. However, the bi-/multi-layers on surfaces 3 and 4 remain because they are encapsulated by graphene monolayers on both sides, which act as a carbon diffusion barrier.[8]

In order to probe the domain size of the graphene, we carried out further characterization using transmission electron microscopy (TEM) (high resolution TEM image in ESI†). We recorded the diffraction patterns at different locations of the sample. There were no discontinuous changes in the orientation of the diffraction spots, indicating that there were no rotational domain boundaries. Results in Fig. 5 show that the diffraction patterns were the same at different locations, suggesting that the monolayer on surface 2 is composed of a large single graphene domain over 200 μm.

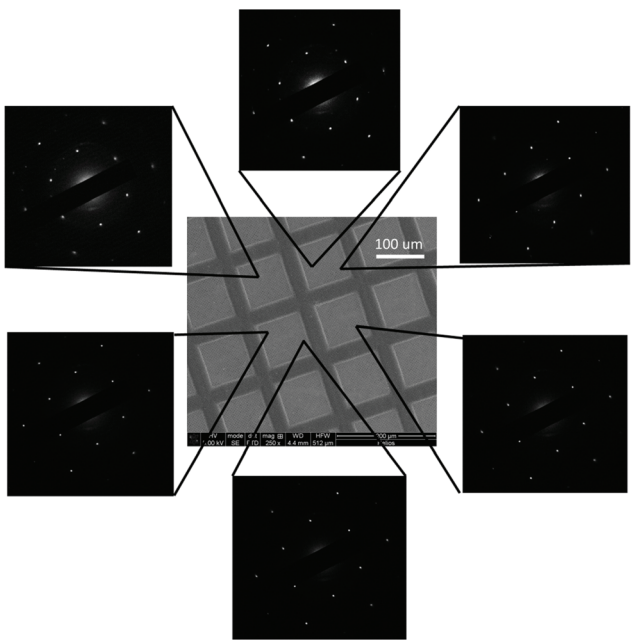

Fig. 5 Large single domain monolayer graphene. The hexagonal diffraction patterns were taken from the corresponding locations on the graphene in the SEM image in the center.

Conclusions

In summary, uniform bi-/multi-layers-free monolayer graphene is obtained using Cu enclosures with a W foil enclosed. The bi-/multi-layers underneath the monolayer graphene are selectively removed while the monolayer remains intact. The W foil plays an important role in maintaining a low carbon content inside of the Cu enclosure by itself absorbing carbon. Both XRD and XPS results indicate the formation of W_2C on the W foil. Finally, using double Cu enclosures, we were able to achieve uniform large-domain graphene with no bi-/multi-layers. The formation of large-area single-domain monolayer graphene can enable large-scale integration of graphene devices with high yield and high reproducibility.

Conflict of interest

The authors declare no competing financial interests.

Acknowledgements

The authors acknowledge the support through the STC Center for Integrated Quantum Materials from NSF (US) grant DMR-1231319. J. K. acknowledges the National Natural Science Foundation of China under award number NSFC (21233001, 21129001).

References

1 A. Reina, X. T. Jia, J. Ho, D. Nezich, H. B. Son, V. Bulovic, M. S. Dresselhaus and J. Kong, *Nano Lett.*, 2009, **9**(1), 30–35.
2 K. S. Kim, Y. Zhao, H. Jang, S. Y. Lee, J. M. Kim, K. S. Kim, J. H. Ahn, P. Kim, J. Y. Choi and B. H. Hong, *Nature*, 2009, **457**(7230), 706–710.
3 X. C. Dong, P. Wang, W. J. Fang, C. Y. Su, Y. H. Chen, L. J. Li, W. Huang and P. Chen, *Carbon*, 2011, **49**(11), 3672–3678.
4 X. S. Li, W. W. Cai, J. H. An, S. Kim, J. Nah, D. X. Yang, R. Piner, A. Velamakanni, I. Jung, E. Tutuc, S. K. Banerjee, L. Colombo and R. S. Ruoff, *Science*, 2009, **324**(5932), 1312–1314.
5 X. S. Li, C. W. Magnuson, A. Venugopal, R. M. Tromp, J. B. Hannon, E. M. Vogel, L. Colombo and R. S. Ruoff, *J. Am. Chem. Soc.*, 2011, **133**(9), 2816–2819.

Published on 05 February 2015. Downloaded by University of California - Santa Barbara on 09/02/2016 05:21:11.

6 N. Petrone, C. R. Dean, I. Meric, A. M. van der Zande, P. Y. Huang, L. Wang, D. Muller, K. L. Shepard and J. Hone, *Nano Lett.*, 2012, **12**(6), 2751–2756.
7 W. Fang, *Bilayer graphene growth by low pressure chemical vapor deposition on copper foil*, S m, Massachusetts Institute of Technology, 2012.
8 S. Nie, W. Wu, S. R. Xing, Q. K. Yu, J. M. Bao, S. S. Pei and K. F. McCarty, *New J. Phys.*, 2012, **14**, 093028.
9 Q. Y. Li, H. Chou, J. H. Zhong, J. Y. Liu, A. Dolocan, J. Y. Zhang, Y. H. Zhou, R. S. Ruoff, S. S. Chen and W. W. Cai, *Nano Lett.*, 2013, **13**(2), 486–490.
10 Y. B. Zhang, T. T. Tang, C. Girit, Z. Hao, M. C. Martin, A. Zettl, M. F. Crommie, Y. R. Shen and F. Wang, *Nature*, 2009, **459**, 820–823.
11 K. S. Novoselov, A. K. Geim, S. V. Morozov, D. Jiang, Y. Zhang, S. V. Dubonos, I. V. Grigorieva and A. A. Firsov, *Science*, 2004, **306**(5696), 666–669.
12 I. Vlassiouk, M. Regmi, P. F. Fulvio, S. Dai, P. Datskos, G. Eres and S. Smirnov, *ACS Nano*, 2011, **5**(7), 6069–6076.
13 S. M. Kim, A. Hsu, Y. H. Lee, M. Dresselhaus, T. Palacios, K. K. Kim and J. Kong, *Nanotechnology*, 2013, **24**(36), 365602.
14 G. H. Han, F. Gunes, J. J. Bae, E. S. Kim, S. J. Chae, H. J. Shin, J. Y. Choi, D. Pribat and Y. H. Lee, *Nano Lett.*, 2011, **11**(10), 4144–4148.
15 S. S. Chen, H. X. Ji, H. Chou, Q. Y. Li, H. Y. Li, J. W. Suk, R. Piner, L. Liao, W. W. Cai and R. S. Ruoff, *Adv. Mater.*, 2013, **25**(14), 2062–2065.
16 X. S. Li, C. W. Magnuson, A. Venugopal, J. H. An, J. W. Suk, B. Y. Han, M. Borysiak, W. W. Cai, A. Velamakanni, Y. W. Zhu, L. F. Fu, E. M. Vogel, E. Voelkl, L. Colombo and R. S. Ruoff, *Nano Lett.*, 2010, **10**(11), 4328–4334.
17 K. Celebi, M. T. Cole, J. W. Choi, F. Wyczisk, P. Legagneux, N. Rupesinghe, J. Robertson, K. B. K. Teo and H. G. Park, *Nano Lett.*, 2013, **13**(3), 967–974.
18 J. H. Lin, W. J. Fang, W. Zhou, A. R. Lupini, J. C. Idrobo, J. Kong, S. J. Pennycook and S. T. Pantelides, *Nano Lett.*, 2013, **13**(7), 3262–3268.
19 W. J. Fang, A. L. Hsu, Y. Song, A. G. Birdwell, M. Amani, M. Dubey, M. S. Dresselhaus, T. Palacios and J. Kong, *ACS Nano*, 2014, **8**(6), 6491–6499.
20 W. Fang, A. L. Hsu, R. Caudillo, Y. Song, A. G. Birdwell, E. Zakar, M. Kalbac, M. Dubey, T. Palacios, M. S. Dresselhaus, P. T. Araujo and J. Kong, *Nano Lett.*, 2013, **13**(4), 1541–1548.
21 D. C. Geng, B. Wu, Y. L. Guo, L. P. Huang, Y. Z. Xue, J. Y. Chen, G. Yu, L. Jiang, W. P. Hu and Y. Q. Liu, *Proc. Natl. Acad. Sci. U. S. A.*, 2012, **109**(21), 7992–7996.
22 N. Liu, L. Fu, B. Y. Dai, K. Yan, X. Liu, R. Q. Zhao, Y. F. Zhang and Z. F. Liu, *Nano Lett.*, 2011, **11**(1), 297–303.
23 H. Kim, C. Mattevi, M. R. Calvo, J. C. Oberg, L. Artiglia, S. Agnoli, C. F. Hirjibehedin, M. Chhowalla and E. Saiz, *ACS Nano*, 2012, **6**(4), 3614–3623.
24 M. Kalbac, H. Farhat, J. Kong, P. Janda, L. Kavan and M. S. Dresselhaus, *Nano Lett.*, 2011, **11**(5), 1957–1963.
25 M. Kalbac, H. Farhat, J. Kong, P. Janda, L. Kavan and M. S. Dresselhaus, *Nano Lett.*, 2011, **11**(5), 1957–1963.
26 X. S. Li, W. W. Cai, L. Colombo and R. S. Ruoff, *Nano Lett.*, 2009, **9**(12), 4268–4272.
27 X. Y. Zhang, L. Wang, J. Xin, B. I. Yakobson and F. Ding, *J. Am. Chem. Soc.*, 2014, **136**(8), 3040–3047.
28 X. R. Wang and H. J. Dai, *Nat. Chem.*, 2010, **2**(8), 661–665.
29 Y. Zhang, Z. Li, P. Kim, L. Y. Zhang and C. W. Zhou, *ACS Nano*, 2012, **6**(7), 6526–6526.
30 Q. K. Yu, L. A. Jauregui, W. Wu, R. Colby, J. F. Tian, Z. H. Su, H. L. Cao, Z. H. Liu, D. Pandey, D. G. Wei, T. F. Chung, P. Peng, N. P. Guisinger, E. A. Stach, J. M. Bao, S. S. Pei and Y. P. Chen, *Nat. Mater.*, 2011, **10**(6), 443–449.
31 P. Y. Huang, C. S. Ruiz-Vargas, A. M. van der Zande, W. S. Whitney, M. P. Levendorf, J. W. Kevek, S. Garg, J. S. Alden, C. J. Hustedt, Y. Zhu, J. Park, P. L. McEuen and D. A. Muller, *Nature*, 2011, **469**(7330), 389–392.
32 O. Akhavan, M. Choobtashani and E. Ghaderi, *J. Phys. Chem. C*, 2012, **116**(17), 9653–9659.
33 F. A. C. Oliveira, J. C. Fernandes, J. M. Badie, B. Granier, L. G. Rosa and N. Shohoji, *Int. J. Refract. Met. Hard Mater.*, 2007, **25**(1), 101–106.
34 F. A. C. Oliveira, B. Granier, J. M. Badie, J. C. Fernandes, L. G. Rosa and N. Shohoji, *Int. J. Refract. Met. Hard Mater.*, 2007, **25**(4), 351–357.
35 S. Dias, F. A. C. Oliveira, B. Granier, J. M. Badie, J. C. Fernandes, L. G. Rosa and N. Shohoji, *Mater. Trans., JIM*, 2007, **48**(5), 919–923.
36 A. A. Voevodin, J. P. O'Neill, S. V. Prasad and J. S. Zabinski, *J. Vac. Sci. Technol., A*, 1999, **17**(3), 986–992.
37 L. Ramqvist, K. Hamrin, G. Johansso, A. Fahlman and C. Nordling, *J. Phys. Chem. Solids*, 1969, **30**(7), 1835–1847.
38 J. Luthin and C. Linsmeier, *Surf. Sci. Spectra*, 2000, **454**, 78–82.
39 Z. Y. Zou, L. Fu, X. J. Song, Y. F. Zhang and Z. F. Liu, *Nano Lett.*, 2014, **14**(7), 3832–3839.

This journal is © The Royal Society of Chemistry 2015